

# **POPDC3 gene variants associate with a new form of limb girdle muscular dystrophy**

John Vissing, MD, DMSc,<sup>1</sup> Katherine Johnson, PhD,<sup>2,3</sup> Ana Töpf, PhD<sup>2</sup>, Shahriar Nafissi, MD,<sup>4</sup> Jordi Díaz-Manera, MD,<sup>5</sup> Vanessa M. French, PhD,<sup>6</sup> Roland F. Schindler, PhD,<sup>6</sup> Padmini Sarathchandra, PhD,<sup>7</sup> Nicoline Løkken, MD,<sup>1</sup> Susanne Rinné, PhD,<sup>8</sup> Max Freund, med stud,<sup>8</sup> Niels Decher, PhD,<sup>8</sup> Thomas Müller, PhD,<sup>9</sup> Morten Duno, PhD,<sup>10</sup> Thomas Krag, PhD,<sup>1</sup> Thomas Brand<sup>†</sup>, PhD,<sup>6</sup> Volker Straub<sup>†</sup>, MD, PhD<sup>2,3</sup>

<sup>†</sup> Shared senior authorship

## **Author affiliations**

<sup>1</sup>Copenhagen Neuromuscular Center, Rigshospitalet, University of Copenhagen, Denmark

<sup>2</sup>John Walton Muscular Dystrophy Research Centre, Institute of Genetic Medicine, Newcastle University and Newcastle Hospitals NHS Foundation Trust, Newcastle upon Tyne, UK

<sup>3</sup>Institute of Cellular Medicine, Newcastle University, Newcastle upon Tyne, UK

<sup>4</sup>Department of Neurology, Iranian Center of Neurological Research, Shariati Hospital, Tehran University of Medical Sciences, Tehran, Iran

<sup>5</sup>Unitat de Malalties Neuromusculars, Servei de Neurologia, Hospital de la Santa Creu i Sant Pau de Barcelona and CIBERER, Spain

<sup>6</sup>Developmental Dynamics, Myocardial Function, National Heart and Lung Institute, Imperial College London, UK

<sup>7</sup>Heart Science Centre, National Heart and Lung Institute, Imperial College London, UK

<sup>8</sup>Institute for Physiology and Pathophysiology, AG Vegetative Physiology, Philipps-University of Marburg, Marburg, Germany

<sup>9</sup>Institute for Molecular Plant Physiology and Biophysics, Julius-von-Sachs Platz 2, 97082 Würzburg, Germany

<sup>10</sup>Department of Clinical Genetics, Rigshospitalet, University of Copenhagen, Denmark

This article has been accepted for publication and undergone full peer review but has not been through the copyediting, typesetting, pagination and proofreading process which may lead to differences between this version and the Version of Record. Please cite this article as doi: 10.1002/ana.25620

Running head: POPDC3 myopathy

Corresponding author:  
John Vissing  
Copenhagen Neuromuscular Center, section 6921  
Rigshospitalet  
Juliane Maries Vej 28  
DK-2100 Copenhagen, Denmark  
Phone: +45 35452562/7357  
E-mail: vissing@rh.dk

## Abstract

**Objective:** The Popeye domain containing 3 (*POPDC3*) gene encodes a membrane protein involved in cAMP signaling. Besides gastric cancer, no disease association has been described. We here describe a new muscular dystrophy associated with this gene.

**Methods:** 1,500 patients with unclassified limb girdle weakness or hyperCKemia were screened for pathogenic *POPDC3* variants. Five patients carrying *POPDC3* variants were examined by muscle MRI, muscle biopsy and cardiac examination. We performed functional analyses in a zebrafish *popdc3* knockdown model and heterologous expression of the mutant proteins in *Xenopus laevis* oocytes to measure TREK-1 current.

**Results:** We identified homozygous *POPDC3* missense variants (p.Leu155His, p.Leu217Phe and p.Arg261Gln) in five patients from three ethnically distinct families. Variants affected highly conserved residues in the Popeye (p.Leu155 and p.Leu217) and carboxy-terminal (p.Arg261) domains. The variants were almost absent from control populations. Probands' muscle biopsies were dystrophic and serum creatine kinase levels were 1,050-9,200 U/L. Muscle weakness was proximal with adulthood onset in most patients, affecting lower earlier than upper limbs. Muscle MRI

revealed fat replacement of paraspinal and proximal leg muscles, while cardiac investigations were unremarkable. Knockdown of *popdc3* in zebrafish, using two different splice-site blocking morpholinos, resulted in larvae with tail curling and dystrophic muscle features. All three mutants cloned in *Xenopus* oocytes caused an aberrant modulation of the mechano-gated potassium channel, TREK-1.

**Interpretation:** Our findings point to an important role of POPDC3 for skeletal muscle function and suggest that pathogenic variants in *POPDC3* are responsible for a novel type of autosomal recessive limb girdle muscular dystrophy.

## Introduction

Autosomal recessively inherited limb girdle muscular dystrophies (LGMD) encompass more than 20 distinct muscular dystrophy subtypes.<sup>1,2</sup> The phenotype of patients with LGMD is heterogeneous, but shares clinical and laboratory findings such as weakness and atrophy of proximal limb muscles, elevated serum creatine kinase (CK) levels and dystrophic findings on muscle biopsy.

Genes involved in currently recognized types of LGMD often affect sarcolemmal glycoproteins, proteins that glycosylate sarcolemmal and scaffolding proteins, and proteins involved in membrane repair and vesicle trafficking in muscle.<sup>3</sup> In 2016, pathogenic variants in *POPDC1*, a member of the new family of proteins encoded by the Popeye domain containing (POPDC) genes, were identified in a family with primary symptoms of cardiac arrhythmia and only mild or no muscle affection (OMIM #616812, LGMDR25, previously classified as LGMD2X).<sup>4</sup> These findings have recently been corroborated in four other individuals from three families.<sup>5</sup> Moreover, variants in the *POPDC2* gene were found to cause AV-block, but no skeletal muscle phenotype, in two families.<sup>6</sup>

The POPDC protein family encompasses three medium-sized, transmembrane proteins, POPDC1, POPDC2 and POPDC3, that are glycosylated to variable extent in different tissues.<sup>7</sup> The proteins and their genes were first described in 1999-2000 and reported to be abundantly expressed in heart and skeletal muscle.<sup>8,9</sup> POPDC proteins have a short extracellular amino terminus, three transmembrane domains, and a conserved Popeye domain that, together with the carboxy-terminal domain (CTD), is localized in the cytoplasmic part of the protein.<sup>10</sup> The Popeye domain functions as a cAMP binding domain, which displays a similar 2D- and 3D-structure, but no homology to other vertebrate cAMP binding proteins at the sequence level.<sup>7</sup> POPDC proteins represent a novel class of cAMP effector proteins, which modulate membrane trafficking of interacting proteins.<sup>7,11</sup> Knockdown of *popdc1* and *popdc2* produces a muscular dystrophy and cardiac arrhythmia phenotype in zebrafish.<sup>4,12</sup> In mouse models, loss of

*Popdc1* and *Popdc2* preferentially exerts effects on the heart, although a regeneration phenotype in skeletal muscle has been described.<sup>13,14</sup>

In this study, we report on the identification of different pathogenic variants in the *POPDC3* gene in three families, leading to a typical LGMD phenotype. We demonstrate an important function of the Popdc3 protein for skeletal muscle in zebrafish, as knockdown of *popdc3* results in a muscle phenotype and in some morphants features of muscular dystrophy. All three *POPDC3* missense variants, when co-expressed with the potassium channel TREK-1 in *Xenopus* oocytes, displayed a loss-of-function phenotype. These findings demonstrate that aberrations in *POPDC3* define a new type of autosomal recessive muscle disease, presenting with a typical LGMD phenotype and no cardiac involvement.

## Materials and Methods

### *Subjects*

Five patients from three families were identified via exome sequencing in a cohort of 1,500 undiagnosed patients with presumed hereditary limb girdle weakness or hyperCKemia. The three families come from Denmark, Iran and Spain (families I, II and III, respectively). The patients had muscle MRI and cardiac studies performed. Muscle biopsies were taken from either the vastus lateralis or tibialis anterior muscles. All patients gave consent to the procedures, which followed institutional guidelines and were in accordance with the Helsinki declaration. Genetic testing was approved by the Newcastle and North Tyneside research ethics committee (REC #09/H0906/28).

### *Molecular genetic analyses of patients*

Variant analysis was performed using whole exome sequencing of leucocyte DNA carried out at the Broad Institute's Genomics Platform<sup>15</sup> and analyzed at the John Walton Muscular Dystrophy Research Centre as part of the MYO-SEQ project. Our initial gene analysis, using standard filtering criteria for rare diseases including minor allele frequency (<0.01), moderate-high variant effect predictor and a gene list comprising 429 genes known to be associated with neuromuscular disease, revealed no candidate variants in the three index cases. We then expanded the analysis to search for new genes that had not been associated with disease before. We added a

deleteriousness filter (combined annotation dependent depletion >20) and a more stringent population frequency parameter (no homozygotes in the control population). Following this, candidate genes were analyzed by Sanger sequencing. Population frequencies were estimated using data from the Genome Aggregation Database (gnomAD).<sup>16</sup>

### ***Cardiac investigations***

A 12-lead ECG was performed in all patients and a 48-hour Holter-monitoring, using a 3-electrode Lifecard CF (Spacelabs Healthcare), was performed in three patients. Echocardiography was performed in all patients in accordance with recommendations from the European Association of Echocardiography and the American Society of Echocardiography.<sup>17</sup> Since cardiac arrhythmias are prominent in patients with variants in *POPDC1* and *POPDC2*,<sup>4,13</sup> patients I-1 and I-2 performed an ECG monitored incremental cycle exercise to provoke cardiac arrhythmias.

### ***MRI of skeletal muscle***

Muscles of the pelvic girdle, thighs and calves were investigated by MRI in all patients. Additionally, lumbar spinal muscle MRI was performed in all patients, except II-1. Axial T1-weighted images were used for qualitative analysis and scored according to the Mercuri scale.<sup>18</sup>

### ***3-D modelling of the POPDC3 molecule***

A 3D model of the POPDC3 protein was generated using PHYRE2 algorithm in intense mode.<sup>19</sup> The resulting PDB file was then refined by energy minimization using the CHARMM refinement tool of the software package Quanta2008 (MSI Accelrys) following the protocol published for modeling of POPDC1.<sup>12</sup>

### ***Muscle histology***



Biopsies were flash-frozen in isopentane cooled by liquid nitrogen and processed using standard histopathological procedures. For immunohistology, we used antibodies against  $\alpha$ -dystroglycan and dystrophin (Leica Biosystems, Wetzlar, Germany) and caveolin-3 (BD, Wokingham, UK). In patient I-1, part of a muscle biopsy was processed for electron microscopy. All procedures have been described previously.<sup>20</sup>

### **Western blotting**

Biopsies from patients I-1 and I-2 were processed for SDS-PAGE and Western blotting as previously described,<sup>21</sup> and incubated with antibodies against POPDC1, POPDC2, POPDC3 (Abcam, Cambridge, UK) and TREK-1 (Sigma-Aldrich, St. Louis, MO) with vinculin (Abcam) as loading control. Goat anti-rabbit horseradish peroxidase was used as a secondary antibody (Thermo Fisher Scientific) and the blots were developed using Clarity Max (Bio-Rad, Hercules, CA).

### **Analysis of TREK-1 current**

*POPDC3* was subcloned into the oocyte expression vector pSGEM. The three variants identified in the human *POPDC3* cDNA were introduced with the QuikChange Site Directed Mutagenesis Kit (Stratagene) according to manufacturer instructions. Oocytes were obtained from anesthetized *Xenopus laevis* frogs and incubated in an OR2 solution containing in mM: NaCl 82.5, KCl 2, MgCl<sub>2</sub> 1, HEPES 5 (pH 7.5) substituted with 2 mg/ml collagenase II (Sigma) to remove residual connective tissue. Subsequently, oocytes were stored at 18 °C in ND96 solution supplemented with 50 mg/l gentamycin, 274 mg/l sodium pyruvate and 88 mg/l theophylline; when indicated the storage solution lacked theophylline. cRNA was synthesized with the HiScribe T7 ARCA mRNA Kit (New England Biolabs) after cDNA linearization with *NheI*. The quality of cRNA was tested using gel electrophoresis and cRNA was

quantified with the NanoDrop 2000 UV-Vis spectrophotometer (Thermo Scientific). Oocytes were each injected with 50 nl of cRNA. TEVC recordings were performed at room temperature (20 - 22 °C) with a TurboTEC 10CD (npi) amplifier and a Digidata 1200 Series (Axon Instruments) as A/D converter. Micropipettes were made from borosilicate glass capillaries GB 150TF-8P (Science Products) and pulled with a DMZ-Universal Puller (Zeitz). Recording pipettes had a resistance of 0.5-1.0 MΩ and were filled with 3 M KCl solution. Recording solution ND96 was composed in mM: NaCl 96, KCl 2, CaCl<sub>2</sub> 1.8, MgCl<sub>2</sub> 1, HEPES 5 (pH 7.5). Data were acquired with Clampex 10 (Molecular Devices) and analyzed with Clampfit 10 (Molecular Devices) and Origin 7 (OriginLab Corporation).

### ***Knockdown of *popdc3* in zebrafish***

Zebrafish AB lines were maintained under standard conditions at 28.5°C according to established protocols,<sup>22</sup> which were approved by the Animal Welfare and Ethical Review Board of the Harefield Heart Science Centre and licensed by the Home Office (PPL 70/7171). When needed, pigmentation was inhibited with 0.2 mM 1-phenyl-2-thiourea (PTU) in egg-water 24 hours post-fertilization. Two splice-blocking antisense morpholino oligonucleotides (Gene Tools, Corvallis, OR, U.S.A.) targeting *popdc3* were used. Morpholino E111 targeted the Exon1/Intron1 splice donor site with the sequence 5-GGTTAATCCACTCACCTGCCTGAAA-3 and I1E2 targeted the Intron1/Exon2 splice-acceptor site with the sequence 5-CACTCGTATCCTGTTTTAGTG ATAA-3. After titration for optimum dosage, 1 ng of E111 or 7 ng of I1E2 were injected into the yolk adjacent to the cell-yolk interface at the 1-2-cell stage of wild-type (WT) embryos. Body curvature phenotypes (axial defects) were evaluated 2 days post-fertilization (dpf) and whole mount F-actin staining using rhodamine-phalloidin (Thermo Fisher Scientific) was performed on 3 dpf embryos. Zebrafish embryos were fixed overnight at 4 °C with 4% paraformaldehyde in phosphate buffered saline (PBS). After extensive washing in PBS, the embryos were equilibrated for 60

minutes in 0.2% Triton X-100/PBS and then incubated with rhodamine-phalloidin (Molecular Probes; 1:20 dilution in 0.2% Triton X-100/PBS) for 90 minutes. Subsequently, the embryos were washed several times in 0.1% Tween20/PBS. Embryos were transferred through a glycerol series (25%, 50%, 80%) before embedding in 80% glycerol for confocal microscopy. For control purposes, injections with standard control morpholino (5'-CCTCTTACCTCAGTTACAATTTATA-3') and co-injections with p53 morpholino 5'-GCGCCATTGCTTTGCAAGAATTG-3' (both from Gene Tools, Corvallis, OR, U.S.A.) were performed. These injections did not cause any pathology (control morpholino) nor were able to rescue the pathological phenotype of *popdc3* morphants. Fluorescence images were acquired using a Zeiss LSM 780 fluorescence confocal microscope (Zeiss, Germany).

A knock-in of the *Popdc3*<sup>R261Q</sup> allele was engineered in zebrafish using CRISPR/Cas9 and introduction of the mutation by homology-directed repair using oligonucleotides carrying the mutation. After intercrossing the F2 offspring, no F3 homozygous mutants could be identified after many attempts. For this study, we therefore had to abandon creating a knock-in model.

## Results

### *Clinical phenotype*

Despite carrying different variants in *POPDC3*, the three ethnically different families shared a similar clinical presentation, with adult-onset weakness of the lower limbs (Table 1). Patients I-1, I-2 and III-2 had calf hypertrophy (Fig 1A). Serum CK levels were elevated to about 3,500 U/L on average (Table 1). The two younger siblings (I-2, III-2) of probands I-1 and III-1 had the same pattern of muscle involvement as the probands, but less severe (Fig 1B). As with the clinical affection, muscle MRI showed fat replacement of muscles in the thighs and prominent fat replacement of the medial gastrocnemii muscles in the probands (Fig 1B and 1C). The gracilis, sartorius and rectus femoris muscles were relatively spared, and in some cases hypertrophied. Spine MRI showed partial fat replacement of the paraspinal muscles in all patients (Fig 1B and 1C). Muscle weakness was clearly proximal, affecting legs more than arms (Fig 1D). None of the five patients had cardiac symptoms or rhythm abnormalities on Holter monitoring and ECG. Incremental cycling to exhaustion provoked no rhythm abnormalities in patients I-1 and I-2. Echocardiography was unremarkable in all patients.

### *Genetic results*

Homozygous variants in the following genes were found in each index case: *ANXA4*, *ZNF638*, *GBA3*, *PCDHGA3*, *POPDC3*, *MGAM*, *CDK12*, *CHAD* and *SNPH* in I-1, *MPP1*, *POPDC3* in II-1 and *EPHA7*, *POPDC3*, *ABCB4*, *BICC1* in III-1. Intersecting these results lead to the identification of biallelic pathogenic variants in a single common gene, *POPDC3* (Table 1). The three variants were missense, affected highly conserved amino acid residues in the carboxy-terminal (c.782G>A, p.Arg261Gln) and Popeye (c.464T>A, p.Leu155His and c.651A>T, p.Leu217Phe) domains of *POPDC3* and were predicted pathogenic by several *in-silico* tools (PolyPhen, SIFT, Mutation Taster and UMD-Prediction). None of the variants were seen in homozygosity in a control

population of >125,000 individuals (<https://gnomad.broadinstitute.org/>), and all their carrier frequencies were very low (0.0004-0.0012%), consistent with being recessive, disease-causing variants.

The variants co-segregated with the disease in the two families where this could be tested (Fig 2). No other likely pathogenic variants in *POPDC3* were found among 1,500 patients with an undefined LGMD phenotype who were assessed for *POPDC3* changes.

#### ***Putative consequences of amino acid substitution***

For each variant, both the affected residue and the neighboring amino acids are highly conserved (Fig 3A), suggesting functional importance. Homology modeling of the POPDC3 protein revealed a location of p.Leu155His and p.Leu217Phe near the hydrophobic core at the top of the cAMP binding pocket, while p.Arg261Gln was located in the CTD (Fig 3B). The location of each mutant residue suggests that p.Leu155His and p.Leu217Phe substitutions could affect proper folding of the Popeye domain or cAMP binding (Fig 3C and 3D), while the p.Arg261Gln variant might have an effect on protein-protein interaction, or opening and closure of the cAMP binding pocket and thereby on the control of cAMP binding, as the mutated residue is close to the cAMP binding pocket (Fig 3E).

#### ***Muscle histology and protein expression***

Muscle biopsies from the three probands and I-2 and III-2 showed features typical for muscular dystrophies, i.e. fibrosis, cell necrosis, large variability in fiber size and whorled fibers (Fig 4A). A considerable variability in histopathology is evident among patients harboring the *POPDC3* gene variants, even among siblings, ranging from moderately to severely affected morphology. In both cases where siblings were affected, the older sibling had a more severe histopathology. The number of internal nuclei was increased but did not resemble a centronuclear myopathy (Fig 4A).

Electron microscopy analysis showed normal ultra-structure of myofibers, nuclei and sarcomeres (Fig 4B).

Immunohistology for  $\alpha$ -sarcoglycan, dystrophin and caveolin-3 showed normal expression in all but III-1, who had an abnormal and varied staining pattern consistent with what is often seen in dystrophic muscle (Fig 4D). No more muscle tissue was left to carry out these analyses in patient II-1.

Western blotting demonstrated a net loss of POPDC3 in both patients tested, more so in the severely affected patient I-1. POPDC1 and POPDC2 expression was decreased in both patients vs. control, while TREK-1 was increased only in the severely affected sibling I-1 (Fig 4C).

#### ***Loss-of-function caused by the three POPDC3 variants***

We have previously described a cAMP-dependent modulation of the  $K_{2P}$  channel TREK-1 by POPDC proteins. To test the functional consequences of the three identified POPDC3 variants, *Xenopus* oocytes were injected with TREK-1 alone or together with wild-type or mutated POPDC3. Unlike the POPDC3<sup>WT</sup>, all three mutants were unable to reduce the current amplitudes of TREK-1, (Fig 5B). In contrast, for p.Leu155His and p.Leu217Phe, TREK-1 currents were even significantly larger than in the absence of POPDC3 (Fig 5B). In the presence of theophylline, a nonspecific phosphodiesterase inhibitor, the TREK-1 modulation by POPDC3<sup>WT</sup> was antagonized/abolished as previously reported for POPDC1 (Fig 5C).<sup>4</sup> Our experiments revealed that the p.Arg261Gln and p.Leu217Phe mutants are still able to bind cAMP, as no significant differences in TREK-1 currents remained after co-expression with these mutants (Fig 5C). In contrast, p.Leu155His apparently does not alter the cAMP affinity of POPDC3, as theophylline did not affect the currents encoded by TREK-1/POPDC3<sup>L155H</sup> (Fig 5B, C).

#### ***Disruption of popdc3 Results in abnormal morphology of zebrafish morphants***

Injection of both E1I1 and I1E2 morpholinos caused characteristic morphological abnormalities at 2 days post fertilization (dpf). *popdc3* morphants displayed a ventral tail curvature as early as 1 dpf, which was absent from wild-type controls (Fig 6A and B, Table 2). Whole-mount staining of 3 dpf embryos with phalloidin and histological analysis demonstrated normal segmentation and myofiber structure in most embryos (Fig 6C-F). However, some *popdc3* morphants displayed dystrophic changes caused by myofiber detachment and disarray (Fig 6G and H). There was no difference in number of centrally positioned myonuclei in *popdc3* morphants vs. wildtype (data not shown).

## Discussion

In this study, we provide evidence for a new type of muscular dystrophy with a limb girdle phenotype, caused by pathogenic variants in the *POPDC3* gene. In a large cohort of patients with limb girdle weakness, we performed exome sequencing and identified three different pathogenic variants in *POPDC3*, causing the same phenotype in ethnically distinct families affected by this new disease. Knockdown of *popdc3* in zebrafish resulted in tail curling and some morphants displayed a muscular dystrophy phenotype. Moreover, forced expression of the putative pathogenic variants in *Xenopus* oocytes revealed aberrant TREK-1 current modulation.

### ***Pathogenicity of identified POPDC3 variants***

The *POPDC3* variants we found in the three families investigated were all missense changes and predicted by numerous *in silico* prediction tools (PolyPhen, Mutation Taster and UMD-Prediction) to be pathogenic, and amongst the top <1% of deleterious variants in the human genome. All variants affected phylogenetic highly conserved residues in critical protein domains of POPDC3. They were extremely rare in large control populations and absent amongst 1,500 undiagnosed patients with muscle disease examined by us. It is also reassuring that the different *POPDC3* variants resulted in a similar clinical and imaging phenotype. The histopathology of the patients demonstrated considerable variability, likely reflecting the impairment of the POPDC3 function inflicted by the variants, but interestingly the ultrastructure of the myofibrils was not affected, suggesting that POPDC3 has probably no sarcomeric function. All three mutant proteins were unable to reduce the current amplitudes of TREK-1, unlike wild-type POPDC3, demonstrating altered functional properties.

### ***POPDC genes and phenotypes***



Mutations in *POPDC1* and *POPDC2* result primarily in a cardiac arrhythmia phenotype,<sup>4,6</sup> while our patients were devoid of cardiac pathology. Although all three POPDC proteins are abundantly expressed in skeletal and cardiac muscle, POPDC3 is more selectively expressed in skeletal muscle compared to the two other POPDC proteins,<sup>8</sup> which may explain the difference in tissue penetrance.

Interestingly, the suppressive effect of POPDC3 on TREK-1 current was abolished in presence of the mutant proteins, suggesting a loss-of-function phenotype. All three POPDC proteins are believed to act as cAMP effectors<sup>13</sup> and findings in the present study also indicated such a function for POPDC3. The POPDC3 variants affected residues located in the Popeye domain or the adjacent CTD, which potentially have an impact on cyclic nucleotide binding or may affect conformational changes of POPDC3 in response to cyclic nucleotide binding. However, no empirically determined protein structure of the Popeye domain is currently available. Therefore, the suspected effects of the mutant POPDC3 proteins rely on a homology model of the Popeye domain and its validity in particular with regard to the functional impact of a single amino acid change is uncertain. The Popeye domain model is based on structural information of bacterial cAMP binding proteins (CRP), which only have limited sequence similarity to the Popeye domain.<sup>13</sup> Thus, there is considerable uncertainty in the prediction of the functional impact of these variants and will require studies of the behaviour of the mutant proteins in their native environment in muscle tissue. We have previously described a cAMP-dependent modulation of the K<sub>2P</sub> channel TREK-1 by POPDC proteins.<sup>4,13</sup> Notably, increasing cAMP levels with theophylline revealed that the p.Arg261Gln and p.Leu217Phe variants are still able to bind cAMP. However, POPDC3<sup>L155H</sup> regulation of TREK-1 was insensitive to raised cAMP levels, indicating that this variant may either affect the cAMP affinity, as we have previously reported for the POPDC1<sup>S201F</sup> variant,<sup>4</sup> or affect for example the ability of the mutant protein of ligand-induced conformational changes. Strikingly, patient II-1 carrying the p.Leu155His variant with an altered cAMP modulation has

the most severe phenotype, displaying as much muscle wasting at age of 36 years as the two other severely affected probands (I-1, III-1), who are in their 50s. We can only speculate about a direct association of the alterations of the TREK-1 current as being relevant for the observed muscle phenotype in our patients, but TREK-1 channels do regulate the functional differentiation of skeletal muscle cells.<sup>23</sup> However, POPDC3, besides regulating TREK-1 channels, might have other, yet unknown functions. They are multi-compartment proteins and, apart from the sarcolemma, are also localized in a variety of other cellular compartments, including caveolae, t-tubules, nuclear envelope and nucleoplasm.<sup>24-26</sup> In cancer, *POPDC1* and *POPDC3* act as tumor suppressors, but it is unknown whether cAMP signaling is required in this functional context.<sup>27,28</sup> Addition of cAMP is able to induce POPDC1 in breast cancer cells and may be involved in the control of cell migration and proliferation in these cells.<sup>29</sup> It is possible that POPDC3 may have a mode of action that is distinct from other POPDC isoforms, which could explain the diverse clinical affection compared to deficiencies caused by mutations of the other two POPDC proteins.<sup>4,6</sup> However, more work needs to be done on the POPDC pathway and interconnection to other pathways as the disease mechanism can be caused by a related secondary single or cascading effect with the mutated POPDC3 as the triggering molecule.

#### ***Zebrafish model indicates important role of POPDC3 for muscle integrity***

In zebrafish *popdc3* morphants, many embryos displayed a curled tail phenotype, which has been described in mutants and morphants of genes involved in ciliopathies.<sup>30</sup> Presently, the relation of the curled tail phenotype to muscular dystrophy remains unclear, however, several morphants of genes causing muscular dystrophy or congenital myasthenic syndrome also display a curled tail similar to the one observed in *popdc3* morphants.<sup>31-34</sup> In addition, we also observed embryos that displayed dystrophic changes in the tail musculature, which were probably caused by

myofiber rupture. Interestingly, myofiber rupture has been observed previously in the case of the zebrafish *popdc1*<sup>S191F</sup> knock-in mutant and in mutants and morphants of genes causing muscular dystrophy.<sup>4,35</sup> It is often the result of disrupted adhesion of muscle fibers to the basal membrane. It is likely, that the phenotype worsens, and the number of affected animals increases as development progresses. Therefore, to study the muscular dystrophy phenotype further, it is planned to introduce the novel *POPDC3* variants into the zebrafish genome with the help of gene editing approaches using CRISPR-Cas9 or TALEN, but as explained in the methods section, this approach has been unsuccessful so far.

#### ***POPDC3 and limb girdle muscular dystrophy***

*POPDC3* associated muscular dystrophy seems to fit a typical LGMD as defined by Walton and Nattrass in 1954 and the LGMD consortium of the European Neuromuscular Centre.<sup>36,37</sup> MRI helped to further characterize the muscle phenotype in our patients. However, *POPDC3*-associated LGMD does not seem to have a specific MR signature, as the selective pattern of pathology found in our patients has also been described in other forms of LGMD.<sup>38,39</sup>

#### ***Conclusions***

The present study characterized three ethnically distinct families with a similar phenotype caused by three homozygous likely pathogenic variants in highly conserved regions of the *POPDC3* gene. *Popdc3*-deficiency in zebrafish embryos disrupted skeletal muscle function as reflected by tail curling and myofiber detachment resulting in muscular dystrophy. In addition, a functional assay demonstrated that the *POPDC3* mutant proteins lost their suppressive activity on TREK-1 current. Collectively, our findings suggest that biallelic variants in the

*POPDC3* gene cause a novel type of autosomal recessive LGMD, and thus defines a novel class of proteins involved in this group of diseases.

Accepted Article

## Acknowledgement

The technical assistance of U. Herbolt-Brand is gratefully acknowledged. Yalda Nilipour, MD, Pediatric Pathology Research Center, Mofid Children Hospital, Shahid Beheshti Medical University (SBMU), Tehran, Iran is acknowledged for providing muscle histology of patient # II-1. The study was supported by grants to Dr. Brand from the British Heart Foundation (PG/14/46/30911, PG/14/83/31128), and the Magdi Yacoub Institute (to T. Brand) and by a Research Grant of the University Medical Center Giessen and Marburg to Dr. Rinné. The MYO-SEQ project was supported by grants to Dr. Straub from Sanofi Genzyme, Ultragenyx, the LGMD2I Research Fund, the Samantha J Brazzo Foundation, the LGMD2D Foundation, the Kurt+Peter Foundation, Muscular Dystrophy UK and the Coalition to Cure Calpain 3.

## Author Contributions

Conception and design of the study: J.V., N.D., V.S., and T.B.

Acquisition and analysis of data; J.V., S.N., V.S., T.B., V.M.F., R.F.S., P.S., A.T., T.K., T.M., S.R., N.D., N.L., M.F., K.J., M.D., and J.D.M.

Drafting the text or preparing the figures: T.B., J.V., S.R., N.D., T.K., T.M., and A.T.

## Potential Conflicts of Interest

All authors report no conflict of interest.

## References

1. Vissing J. Limb girdle muscular dystrophies: classification, clinical spectrum and emerging therapies. *Curr Opin Neurol* 2016;29: 635-641.
2. Thompson R, Straub V. Limb-girdle muscular dystrophies: international collaborations for translational research. *Nat Rev Neurol* 2016;12:294-309.
3. Liewluck T, Milone M. Untangling the complexity of limb-girdle muscular dystrophies. *Muscle Nerve* 2018;doi:10.1002/mus.26077.
4. Schindler RF, Scotton C, Zhang J, et al. POPDC1<sup>S201F</sup> causes muscular dystrophy and arrhythmia by affecting protein trafficking. *J Clin Invest* 2016;126:239-253.
5. De Ridder W, Nelson I, Asselbergh B, et al. Muscular dystrophy with arrhythmia caused by loss-of-function mutations in BVES. *Neurol Genet* 2019;5:e321.
6. Rinné S, Ortiz-Bonnin B, Stallmeyer B, et al. Conduction disorder caused by a mutation in *POPDC2*, a novel modulator of the cardiac sodium channel SCN5A. *Acta Physiol* 2016;216(S707):0S03-1. (abstract)
7. Brand T, Schindler R. New kids on the block: The Popeye domain containing (POPDC) protein family acting as a novel class of cAMP effector proteins in striated muscle. *Cell Signal* 2017;40:156-165.
8. Andrée B, Hillemann, T, Kessler-Icekson G, et al. Isolation and characterization of the novel popeye gene family expressed in skeletal muscle and heart. *Dev Biol* 2000;223:371-382.
9. Reese DE, Zavaljevski M, Streiff NL, et al. A novel gene expressed during coronary blood vessel development. *Dev Biol* 1999;209:159-171.

10. Brand T, Simrick SL, Poon KL, et al. The cAMP-binding Popdc proteins have a redundant function in the heart. *Biochem Soc Transact* 2014;42:295-301.
11. Schindler RF, Brand T. The Popeye domain containing protein family-A novel class of cAMP effectors with important functions in multiple tissues. *Prog Biophys Mol Biol* 2016;120:28-36.
12. Kirchmaier BC, Poon KL, Schwerte T, et al. The Popeye domain containing 2 (popdc2) gene in zebrafish is required for heart and skeletal muscle development. *Dev Biol* 2012;363:438-450.
13. Froese A, Breher SS, Waldeyer C, et al. Popeye domain containing proteins are essential for stress-mediated modulation of cardiac pacemaking in mice. *J Clin Invest* 2012;122:1119-1130.
14. Andrée B, Fleige A, Arnold HH, et al. Mouse Pop1 is required for muscle regeneration in adult skeletal muscle. *Mol Cell Biol* 2002; 22:1504-1512.
15. Johnson K, Töpf A, Bertoli M, et al. Identification of GAA variants through whole exome sequencing targeted to a cohort of 606 patients with unexplained limb-girdle muscle weakness. *Orphanet J Rare Dis* 2017;12:173.
16. Karczewski KJ, Francioli LC, Tiao G, Cummings BB, Alföldi J, Wang Q, et al. Variation across 141,456 human exomes and genomes reveals the spectrum of loss-of-function intolerance across human protein-coding genes. *bioRxiv*  
doi: <https://doi.org/10.1101/531210>
17. Lang RM, Bierig M, Devereux RB, et al. Recommendations for chamber quantification. *Eur J Echocardiogr* 2006;7:79-108.

18. Mercuri E, Pichiecchio A, Allsop J, Messina S, et al. Muscle MRI in inherited neuromuscular disorders: past, present, and future. *J Mag Res Imag* 2017;25:433-440.
19. Kelley LA, Mezulis S, Yates CM, et al. The Phyre2 web portal for protein modeling, prediction and analysis. *Nat Protoc* 2015;10:845-858.
20. Krag T, Ruiz CR, Vissing J. Glycogen synthesis in glycogenin 1 deficient patients; a role for glycogenin 2 in muscle. *J Clin Endo Metab* 2017;102:2690-2700.
21. Krag TO, Pinós T, Nielsen TL, et al. Differential muscle involvement in mice and humans affected by McArdle disease. *J Neuropathol Exp Neurol* 2016;75:441-454.
22. Westerfield M. *The zebrafish book: a guide for the laboratory use of zebrafish Danio (Brachydanio rerio)*. Eugene, Oregon, USA: University of Oregon Press 2003.
23. Afzali AM, Ruck T, Herrmann AM, et al. The potassium channels TASK2 and TREK1 regulate functional differentiation of murine skeletal muscle cells. *Am J Physiol Cell Physiol* 2016;311:C583-C595.
24. Soni S, Raaijmakers AJA, Raaijmakers LM, et al. A proteomics approach to identify new putative cardiac intercalated disk proteins. *PLoS One* 2016;11: e0152231.
25. Wilkie GS, Korfali N, Swanson SK, et al. Several novel nuclear envelope transmembrane proteins identified in skeletal muscle have cytoskeletal associations. *Mol Cell Proteomics* 2011;10:M110 003129.
26. Schindler RF, Scotton C, French V, et al. The popeye domain containing genes and their function in striated muscle. *J Cardiovasc Dev Dis* 2016;3:22.



27. Luo D, Lu ML, Zhao GF, et al. Reduced Popdc3 expression correlates with high risk and poor survival in patients with gastric cancer. *World J Gastroenterology* 2012;18:2423-429.
28. Kim M, Jang HR, Haam K, et al. Frequent silencing of popeye domain-containing genes, BVES and POPDC3, is associated with promoter hypermethylation in gastric cancer. *Carcinogenesis* 2010;31:1685-1693.
29. Amunjela J, Tucker S. Dysregulation of POPDC1 promotes breast cancer cell migration and proliferation. *Biosci Rep.* 2017;37.
30. Song Z, Zhang X, Jia S, et al. Zebrafish as a model for human ciliopathies. *J Genet Genomics* 2016;43:107-120.
31. Parsons MJ, Campos I, Hirst EM, et al. Removal of dystroglycan causes severe muscular dystrophy in zebrafish embryos. *Development* 2002;129:3505-3512.
32. Nixon SJ, Wegner J, Ferguson C, et al. Zebrafish as a model for caveolin-associated muscle disease; caveolin-3 is required for myofibril organization and muscle cell patterning *Hum Mol Genet* 2005;14:1727–1743.
33. Thornhill P, Bassett D, Lochmüller H, et al. Developmental defects in a zebrafish model for muscular dystrophies associated with the loss of fukutin-related protein (FKRP). *Brain* 2008;131:1551–1561.
34. O'Connor E, Töpf A, Müller JS, et al. Identification of mutations in the *MYO9A* gene in patients with congenital myasthenic syndrome. *Brain* 2016; 139:2143–2153.

35. Goody MF, Carter EV, Kilroy EA, et al. "Muscling" throughout life integrating studies of muscle development, homeostasis, and disease in zebrafish. *Curr Top Dev Biol* 2017;124:197-234.
36. Walton JN, Nattrass FJ. On the classification, natural history and treatment of the myopathies. *Brain* 1954;77:169-231.
37. Straub V, Murphy A, Udd B on behalf of the 229<sup>th</sup> ENMC workshop study group. 229<sup>th</sup> ENMC international workshop: Limb girdle muscular dystrophies – nomenclature and reformed classification, 17-19 March 2017, Naarden, The Netherlands. *Neuromuscul Disord* 2018;28(8):702-710.
38. Díaz-Manera J, Llauger J, Gallardo E, et al. Muscle MRI in muscular dystrophies. *Acta Myol* 2015;34:95-108.
39. Sarkozy A, Deschauer M, Carlier RY, et al. Muscle MRI findings in limb girdle muscular dystrophy type 2L. *Neuromuscul Disord* 2012;22 Suppl 2:S122-9.

**Table 1: Demographics, and clinical and laboratory findings in five patients with POPDC3 myopathy.**

| Family-patient # | Sex (F/M)/age (yrs) | Onset age (yrs) | Nature of onset          | Holter/ECG, cardiac echo  | Creatine kinase levels: | Homozygous variants: Nucleotide/protein |
|------------------|---------------------|-----------------|--------------------------|---------------------------|-------------------------|---|
| I-1              | M/50                | 40              | Falls, poor runner       | LVEF=55%<br>Holter normal | 2,000-9,227             | c.782G>A,<br>p.Arg261Gln                |
| I-2              | F/42                | Teens           | Poor runner              | Normal                    | 1,200-1,770             | c.782G>A,<br>p.Arg261Gln                |
| II-1             | M/36                | 25              | Poor runner              | Normal                    | 1,050-7,650             | c.464T>A,<br>p.Leu155His                |
| III-1            | M/59                | 20              | Poor runner              | Normal                    | 2,000-4,500             | c.651A>T<br>p.Leu217Phe                 |
| III-2            | M/57                | 35              | Atrophy of gastrocnemius | Normal                    | 4,000-6,000             | c.651A>T<br>p.Leu217Phe                 |

Upper reference for normal creatine kinase is 200. F = female, M = male, yrs = years, LVEF = left ventricular ejection fraction.

Table 2: Axial defects in zebrafish *popdc3* morphants at 2-3 dpf

|                | n   | normal                     | mild                     | mod.                        | severe                     |
|----------------|-----|----------------------------|--------------------------|-----------------------------|----------------------------|
| <b>control</b> | 563 | 532<br>94.5%               | 15<br>2.7%               | 9<br>1.6%                   | 7<br>1.2%                  |
| <b>E1I1-MO</b> | 238 | 195 <sup>ns</sup><br>81.9% | 20 <sup>**</sup><br>8.4% | 18 <sup>**</sup><br>7.6%    | 5 <sup>ns</sup><br>2.1%    |
| <b>I1E2-MO</b> | 376 | 48 <sup>***</sup><br>12.8% | 35 <sup>ns</sup><br>9.3% | 255 <sup>***</sup><br>67.8% | 38 <sup>***</sup><br>10.1% |

ns = non-significant, mod. = moderate, \*\* p<0.01, \*\*\* p<0.001 vs. control

## Figure legends

**Figure 1. Muscle affection in patients with *POPDC3* gene variants on clinical examination and muscle MRI. (A)** Calf hypertrophy in two patients (asymmetric in III-2). In patient III-1, there is pectoral and biceps muscle atrophy. **(B)** MRI shows pronounced replacement of muscle by fat in paraspinal, thigh muscle and medial gastrocnemius muscles. **(C)** Muscle fat replacement on MRI was scored with the Mercuri scale (1 = normal and 4 = severe involvement, end-stage with complete replacement by fat). **(D)** Muscle strength in different muscle groups of the five patients. Values are mean  $\pm$  SE.

**Figure 2. Pedigrees of the three involved families.** Parents of patients were consanguineous in all families. In the Iranian family, only the proband II-1, identified as homozygous for the p.Leu155His variant, was available for testing. In the Danish family, two (I-1 and I-2) of four siblings were identified as homozygous for the p.Arg261Gln variant, while in the Spanish family, two (III-1 and III-2) of five siblings were homozygous for the p.Leu217Phe variant. All the unaffected individuals (parents and siblings) tested were heterozygous for their respective variants.

**Figure 3. Localization of residues affected by variants in the *POPDC3* protein. (A)** Evolutionary conservation of residues affected by the three variants discovered in patients. Identical residues are labelled in yellow and similar residues in green, while non-conserved residues are turquoise. **(B)** 3D homology model of the *POPDC3* protein. The extracellular domain (ECD), the three transmembrane domains (TM1-3), the nucleotide-binding Popeye domain (marked in cyan) and the C-terminal domain (CTD colored in orange) are shown. The cAMP molecule (ball-and-stick model in

green), the invariant sequence motifs DSPE and FQVT (C-atoms colored in light blue) involved in nucleotide binding and the three sites of substitutions (indicated as red spheres) are marked. All changes described here are located near the cAMP binding site, which is demarcated by the conserved DSPE....FQVT sequence motif (colored in blue). **(C and D)** Mutation of **(C)** Leu155 to histidine, and **(D)** Leu217 to phenylalanine results in bad van der Waals contacts, e.g. with Trp186 and Trp212, due to the larger sidechains of the amino acid introduced (carbon atoms in magenta) and their dense packing within the surrounding hydrophobic core. This very likely leads to structural changes in and nearby the cAMP binding site and might therefore reduce the binding affinity of the mutant protein for cAMP. **(E)** Detailed view of the area surrounding residue 261, which is located on the surface of the carboxy-terminal domain (CTD). While in the model the distance between Arg261 and the cAMP molecule seems rather large, Arg261 could still be involved in nucleotide binding. By forming ion charge pair with Asp238 and Asp241 it might regulate the opening and closing of the nucleotide binding pocket through altering the location of helix  $\alpha_7$ , which is placed above the cAMP moiety. Alternatively, it could be involved in protein-protein interaction as it forms a highly conserved DIR motif together with two adjacent residues (D259 and I260). Substitution of Arg261 by glutamine disrupts these interactions.

**Figure 4. Histopathologic and functional effects of *POPDC3* variants.** **(A)** Muscle involvement is evident in the probands (I-1, II-1, III-1), with central nuclei, fibrosis and necrotic fibers. **(B)** Transmission electron microscopy of I-1 demonstrates a normal microfibrillar structure as seen in a cross-section. Central nuclei appear as normally seen in regenerating myofibers. Sarcomere structure appears normal with Z-line in register and normal distribution of mitochondria and sarcoplasmic reticulum. **(C)** Western blot analysis of protein expression in patient and control (Ctrl) muscle biopsies. Patients expressed less POPDC1/2/3 than a healthy control

while an increase in TREK-1 was also seen in I-1. (D) Immunohistological stains for  $\alpha$ -sarcoglycan ( $\alpha$ SG), dystrophin (DYS) and caveolin 3 (Cav3) on muscle sections demonstrate a near normal stain in all patients, but III-1, who has a reduced level of dystrophin and caveolin 3 in some fibers. Bar in light microscopy images is 50 $\mu$ m.

**Figure 5: Modulation of TREK-1 by wild-type and mutant POPDC3.**

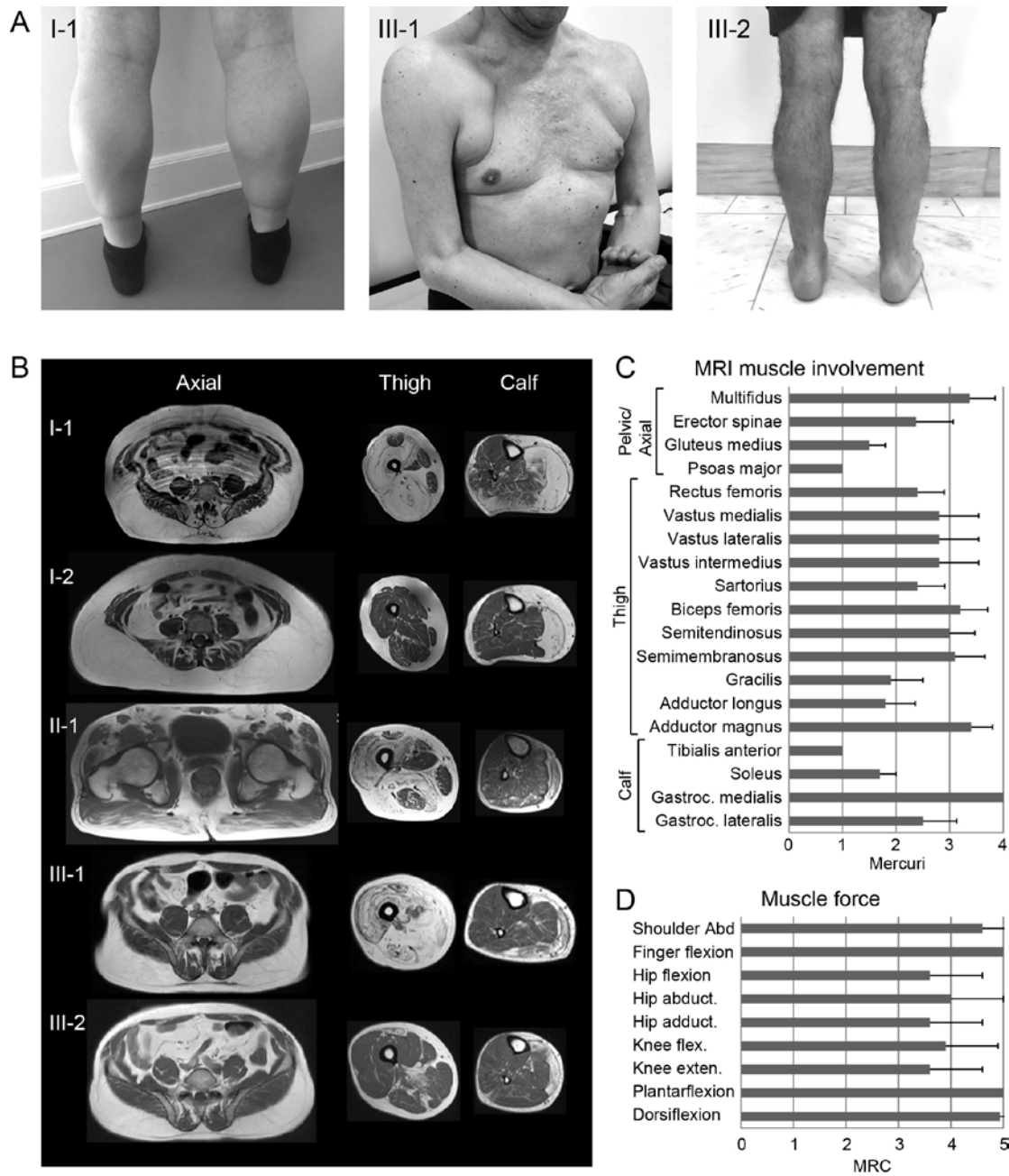
TREK-1 cRNA (0.25 ng) was injected alone or co-injected with POPDC3 (1.25 ng) or mutant POPDC3<sup>R261Q</sup>, POPDC3<sup>L217F</sup> or POPDC3<sup>L155H</sup> (1.25 ng) in *Xenopus laevis* oocytes which were subsequently placed in a theophylline-free storage solution. (A) Depicted are representative current traces measured at a voltage step to +40 mV from a holding potential of -80 mV 24 h after injection. (B) Relative current amplitudes (normalized to TREK-1 injected alone) analyzed at +40 mV, 24 h after injection. The numbers of individual oocytes recorded (n) from three to six independent batches (N = 3-6) are provided within the respective bar graphs. (C) Experiments as described above (A-B) and with similar amounts of injected cRNAs, but oocytes were incubated in storage solution containing theophylline. Data are presented as mean  $\pm$  s.e.m. \*\*, indicates  $p < 0.01$ ; \*\*\*,  $p < 0.001$ ; ns, not significant.

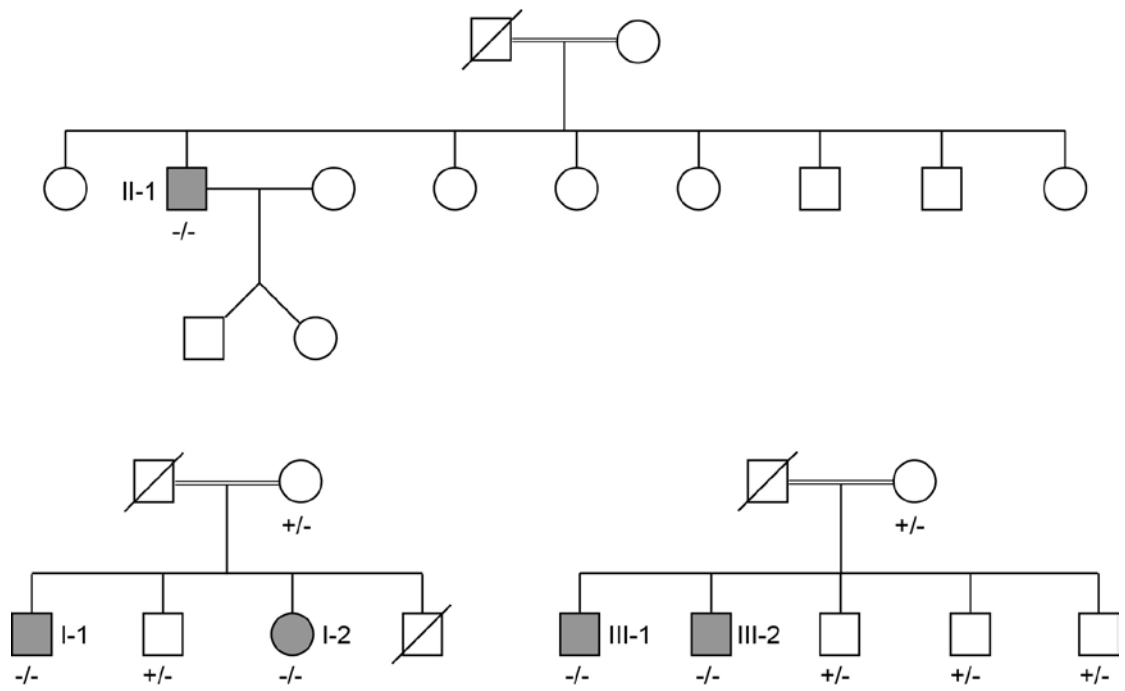
**Figure 6. *popdc3* knockdown in zebrafish results in a muscular dystrophy**

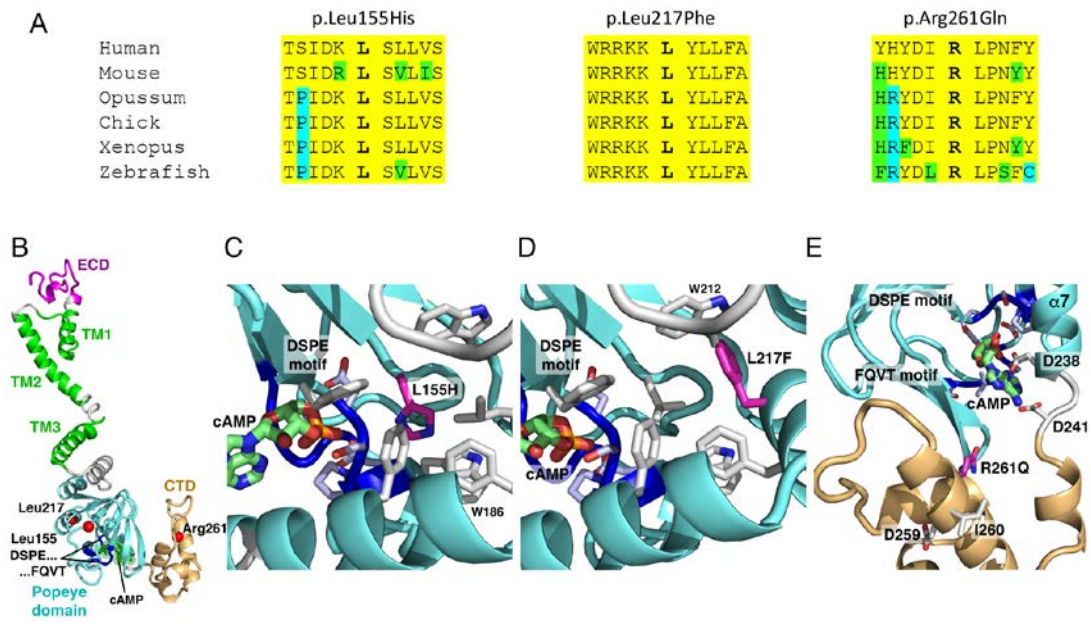
**phenotype.** (A and B) healthy control zebrafish embryos display a straight tail (A), whereas, a majority of *popdc3* morphants display a characteristic, curly tail (B). (C and D) Rhodamine phalloidin whole mount-stained tail of a 3dpf healthy control (C) and *popdc3* knockdown (D) zebrafish embryo. The areas demarcated by the white boxes are enlarged in panels E and F to highlight the normal myofibrillar structure in

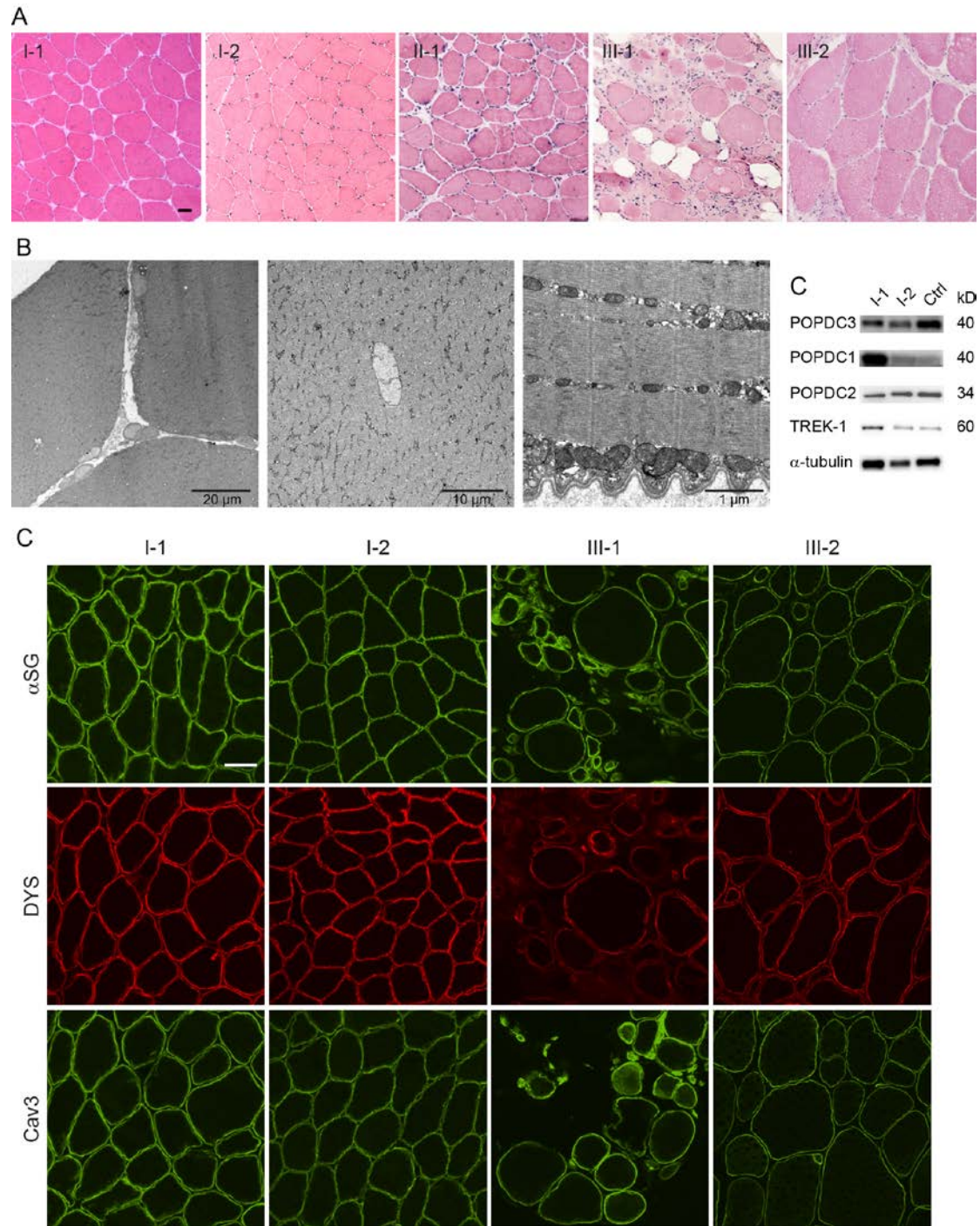
most embryos. (**G** and **H**) in comparison to the regular structure of the myotome seen in control embryos (**G**), some *popdc3* morphant embryos (**H**) display a muscular dystrophy phenotype characterized by areas devoid of myofibers (asterisks), which is probably caused by myofiber rupture (arrows).

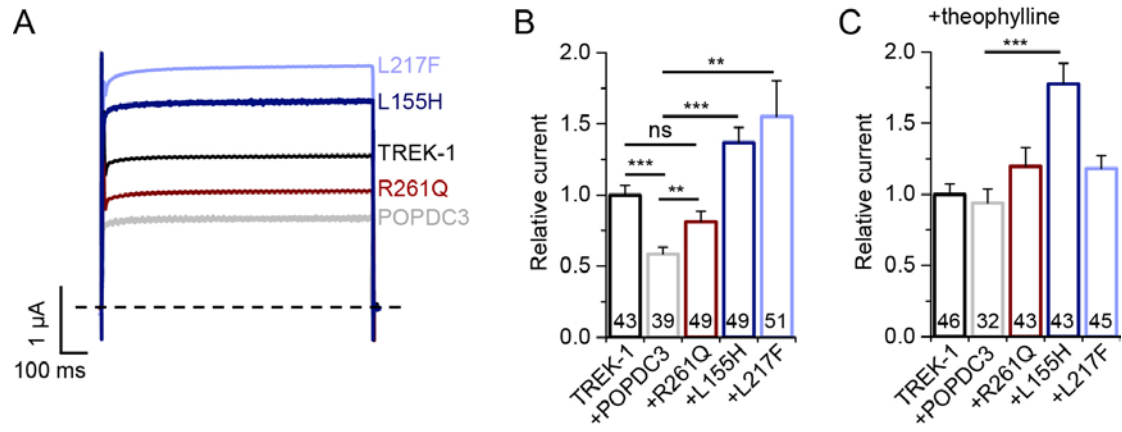












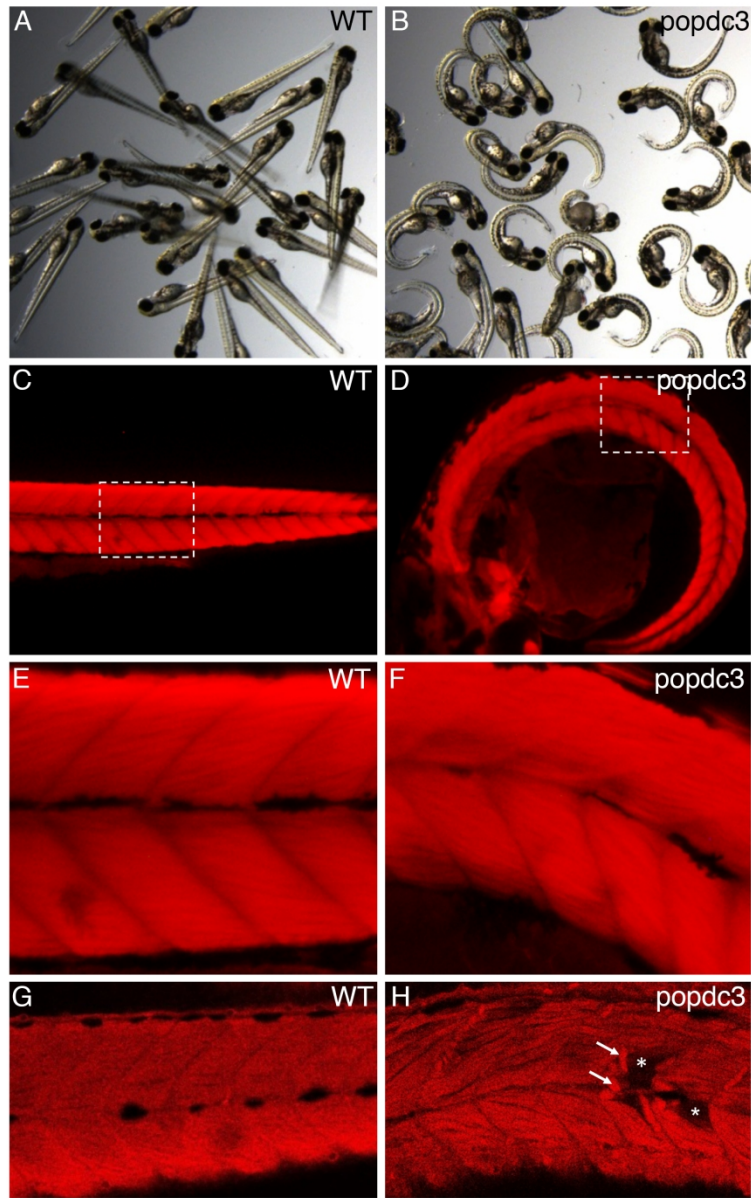


Figure 6